

Aggregation-Induced Emission

Dinitriles Bearing AIE-Active Moieties: Synthesis, E/Z Isomerization, and Fluorescence Properties**

Thiago Teixeira Tasso, Taniyuki Furuyama, and Nagao Kobayashi*[a]

Abstract: Dinitriles bearing aggregation-induced emission (AIE)-active moieties [tetraphenylethylene (TPE) or diphenylphenanthrene (DPP)] were prepared. Compounds **4** (TPE-linked) and **8** (DPP-linked) showed considerably redshifted emission resulting from their large Stokes shifts and also strong fluorescence in the aggregated and solid states. Pure *E* and *Z* stereoisomers of both dinitriles were easily separated,

and their isomerization equilibria and fluorescence properties were investigated. In addition to their pronounced AIEE behavior, **4** and **8** also showed various reversible chromic responses to external stimuli, namely, solvato-, piezo-, vapo-, and thermochromism, which make them potential candidates for smart materials.

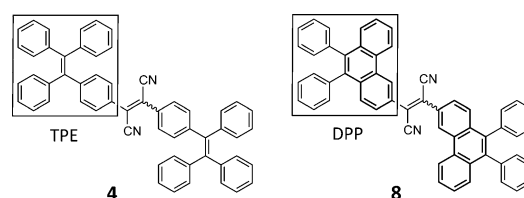
Introduction

The demand for next-generation dyes that can effectively absorb and emit light in the near-infrared (NIR) region has increased recently due to their applicability in solar cells,^[1] as probes for bioimaging,^[2] and as photosensitizing agents.^[3] In this regard, π -conjugated organic compounds are good candidates, since their properties can be fine-tuned by means of appropriate synthetic modifications. Redshifted absorption/emission can be achieved by lowering the energy gap between the HOMO and LUMO levels of the chromophores through extension of the π conjugation^[4] and/or modification with push-pull substituents.^[5] However, most π -conjugated planar fluorophores suffer from aggregation-caused quenching, in which their emission in the solid state is completely quenched due to formation of excimers.^[6] This is a serious limitation to their applicability in imaging and efficiency in photovoltaic devices such as OLED displays, since strong luminescence in the solid/aggregate state is crucial for proper color contrast in these fields.

Recently, a new class of chromophores showing weak emission in solution and strong emission in the solid state owing to aggregation-induced emission (AIE) behavior was discovered,^[7] and this opened the way for the design of improved compounds and advanced materials.^[8] The tetraphenylethylene (TPE) moiety has been widely used for the design of AIE-active compounds due to its ease of preparation and outstanding AIE effect.^[6a] The rotatable phenyl rings are responsible for nonradiative deactivation of the excited state in solution, whereas

on aggregation intramolecular rotations become restricted and the radiative channel is opened. Furthermore, the propeller-shaped orientation of the phenyl rings imposes severe steric hindrance on the chromophore unit, which prevents π - π aggregation and fluorescence quenching. In most cases, however, TPE-modified fluorophores show blue/green fluorescence^[9] due to small π conjugation and absence of intramolecular charge-transfer transitions.

In an attempt to obtain novel AIE fluorophores with redshifted absorption/emission, we designed the TPE-modified dinitrile **4** (Scheme 1). The vinylene bridge is expected to expand the overall π conjugation of the molecule by communicating be-



Scheme 1. Molecular structures of dinitriles **4** and **8**.

tween the TPE moieties, while the two cyano groups can enhance its polarizability to result in large Stokes shifts, and thus their emission may occur at lower energy. Since the fluorescence turn-on of AIE-active chromophores is directly related to the rotational freedom of the phenyl rings in the packing structure, we also synthesized dinitrile **8** containing diphenylphenanthrene (DPP) moieties. DPP is a TPE analogue in which two of the four benzene rings are locked by a covalent bond to form a phenanthrene unit. The photophysical properties of partially locked TPE derivatives have already been reported,^[10] but these studies were limited to simple model molecules,

[a] T. T. Tasso, Dr. T. Furuyama, Prof. Dr. N. Kobayashi
Department of Chemistry, Graduate School of Science
Tohoku University, Sendai, 980-8578 (Japan)
E-mail: nagaok@m.tohoku.ac.jp

[**] AIE: aggregation-induced emission.

Supporting information for this article is available on the WWW under
<http://dx.doi.org/10.1002/chem.201406128>.

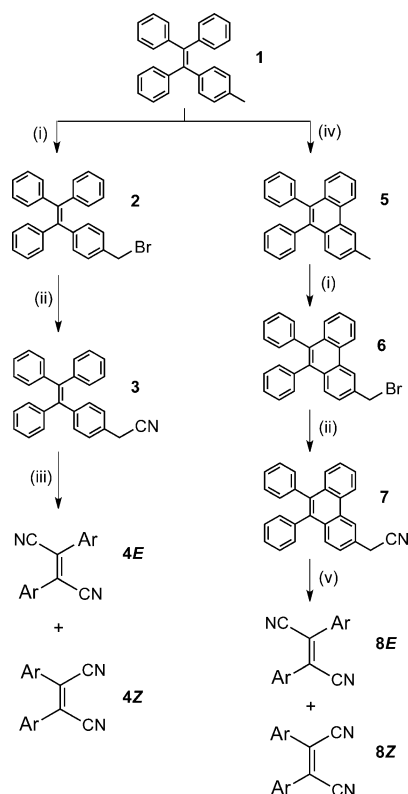
mainly to verify the restriction of intramolecular rotation mechanism.

Herein, we show that phenyl locking in expanded structures such as dinitriles **4** and **8** can lead to intriguing differences in the properties of these compounds. Since the *E/Z* isomers of both **4** and **8** could be easily separated by conventional column chromatography, we also investigated their photo-physical properties separately. This is a rare case in the chemistry of AIE-active chromophores, since the isolation of stereoisomers of TPE derivatives is rather difficult.^[11] Not only different fluorescence profiles, but also distinct chromic responses to external stimuli, were found for the stereoisomers of **4** and **8**. Hence, we believe our work can further contribute to enriching the understanding of the AIE phenomenon.

Results and Discussion

Synthesis

The synthetic route for dinitriles **4** and **8** is shown in Scheme 2. Compounds **3** and **7** were prepared by the Kolbe nitrile synthesis, followed by dimerization in the presence of a strong base. This is a conventional procedure for the preparation of dinitriles due to its straightforward steps and moderate to good yields.^[12] Dinitriles **4** and **8** were obtained as mixtures of *E* and *Z* isomers. Oxidation of the TPE unit of **1** generated the



Scheme 2. Synthesis of the compounds studied in this work. Reagents and conditions: i) NBS, benzoyl peroxide, CCl_4 , reflux, overnight; ii) KCN, DMSO, 90°C , 2 h; iii) NaOMe, I_2 , diethyl ether, 0°C , 30 min; iv) 2,3-dichloro-5,6-dicyanobenzoquinone, MeSO_3H , CH_2Cl_2 , 0°C , 30 min; v) NaOMe, I_2 , THF, -35°C , 10 min.

DPP derivative **5** as the sole product, since the methyl group is responsible for regioselective oxidation of the closest phenyl ring.^[13] To illustrate this, the same oxidative reaction was carried out with compound **3** as precursor, and a mixture of two isomers was obtained in a 6:1 ratio (Scheme S1 in the Supporting Information), as confirmed by ^1H NMR spectroscopy. This is explained by the electron-withdrawing nature of the cyano group, which removes electron density from the closest phenyl rings, making it more favorable for the reaction to occur on the opposite side of the TPE moiety.

There are very limited reports on the distinct AIE behavior of pure *E/Z* stereoisomers, due to the difficulty of the separation step. Long alkyl chains can be attached to a TPE derivative to increase the size of the molecule and facilitate the separation of stereoisomers, as shown by Tang and co-workers.^[11a] However, the crystallinity of the pure isomers was lowered by the long alkyl chains, and this prevented their characterization in the solid state by single-crystal X-ray analysis. In our case, pure *E* and *Z* isomers of both **4** and **8** were easily separated by simple chromatography on silica gel without any modification of the molecular structure. The structures of the pure isomers were also unambiguously elucidated by single-crystal X-ray diffraction (see below).

E/Z Photoisomerization in Solution

The distinct ^1H NMR spectra of **4** and **8** allowed their unambiguous characterization, as well as a clear investigation of the *E/Z* isomerization process (Figure 1). Peaks of **4Z** at about $\delta = 7.06$ and 6.95 ppm (Figure 1 d) are absent for **4E**, and the low-field doublet at $\delta = 7.54$ ppm is exclusive to the latter (Figure 1 a). In the spectra of **8**, on the other hand, the phenanthrene proton signals are considerably shifted to low field compared to the phenyl protons, and larger chemical shifts are observed for the *E* form. *E/Z* isomerization on UV irradiation is commonly observed in olefins, and a detailed study on this kind of equilibrium is important to obtain information about the stability of the stereoisomers.^[14]

To obtain quantitative data for the isomerization equilibria of **4** and **8**, the sample concentration, distance from the UV lamp, and time of irradiation were fixed. Starting from solutions of pure *E* and *Z* isomers, the isomerization reaction clearly proceeded for both **4** and **8**, as shown in Figure 1 and the Supporting Information (Figures S1 and S2). The interconversion rates were initially fast at the beginning and noticeable even in the first minutes of irradiation, and slowed down until equilibrium was reached (Figure 2). Interestingly, not only were the isomerization kinetics approximately twice as fast for **8** (ca. 90 min) compared to **4** (ca. 180 min), but also the final mixture differed from the 50/50 *E/Z* ratio in both cases. When equilibrium was reached, the *E/Z* ratios found for **4** and **8** were 59/41 and 46/54, respectively, that is, the most stable stereoisomer is also different for these dinitriles. No isomerization was observed on irradiation of the samples with light in the solid state, due to the locked conformation of the compounds in the packing structure. To further support the observed results, we carried out theoretical calculations on the total energy of

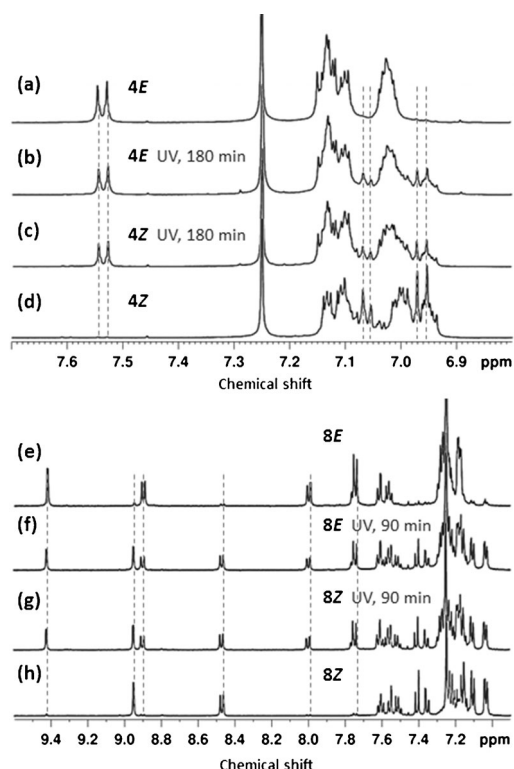


Figure 1. Top: ¹H NMR spectra of CDCl₃ solutions of **4E** and **4Z** before (a, d) and after UV irradiation for 180 min (b, c). Bottom: ¹H NMR spectra of CDCl₃ solutions of **8E** and **8Z** before (e, h) and after UV irradiation for 90 min (f, g).

the molecules (see Supporting Information for details). The difference in Gibbs free energy of the *E* and *Z* isomers ($\Delta G = G_E - G_Z$) for **4** was found to be $-0.58 \text{ kcal mol}^{-1}$, which indicates a slightly higher thermodynamic stability of the *E* form. In contrast, the positive ΔG value of $28.4 \text{ kcal mol}^{-1}$ found for **8** suggests higher stability of the *Z* isomer. These trends support the experimental data obtained by ¹H NMR spectroscopy.

Photophysical Properties in Solution

The AIE behavior of the stereoisomers was investigated in THF/water (Figure 3 and Figure S3 in the Supporting Information). The dinitriles are emissive to some extent in pure THF solution, with a broad emission peak around 640 nm for **4** and 560 nm for **8**. The fluorescence intensity of nitriles **4E** and **4Z** decreased progressively with increasing fraction of water in the mixtures, due to the increase in the polarity of the medium. In mixtures containing 60% water, the fluorescence peak was blueshifted and the intensity sharply increased with increasing water content, until a maximum quantum yield Φ_F of about 40% was reached in pure water, which is similar to the Φ_F values found in the solid state (see above). This indicates that the molecules aggregate with increasing amount of poor solvent above 60%; this prevents rotation of the phenyl rings and opens

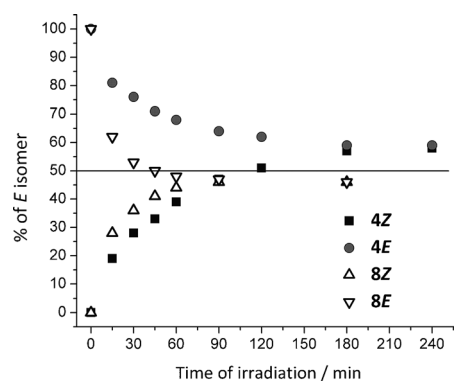


Figure 2. Plot of the percentage of *E* isomer present in solutions of the dinitriles after each UV irradiation interval.

up the fluorescence pathway. The 12-fold increase in the Φ_F values of **4E** and **4Z** that was observed on aggregation in solution confirms the aggregation-induced emission enhancement (AIEE) behavior (Supporting Information, Figure S4). Dinitriles **8E** and **8Z**, on the other hand, showed almost constant emission efficiency up to 80% water, followed by a sharp increase in fluorescence for the mixture with 99% water. An approximate fourfold increase in Φ_F was observed for **8E** and **8Z**, which thus show a weaker AIEE effect compared to **4**.

Compounds **4** and **8** are composed of TPE/DPP and CN units, which act as electron-donating and electron-accepting moieties, respectively. This push-pull structure results in transitions with strong intramolecular charge-transfer (CT) character, which can be tuned by varying the polarity of the solution. With this in mind, we investigated the absorption and emission spectra of these compounds in a series of solvents, as shown in Figure 4A and B for **4E** and **8Z** and Figure S5 of the

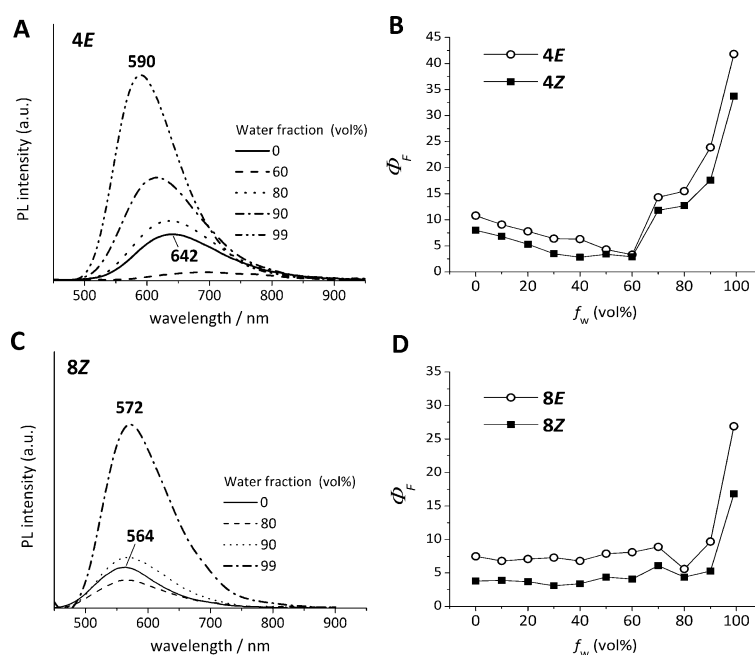


Figure 3. Fluorescence spectra of A) **4E** and C) **8Z** and fluorescence quantum yields Φ_F of B) **4E/4Z** and D) **8E/8Z** in water/THF mixtures.

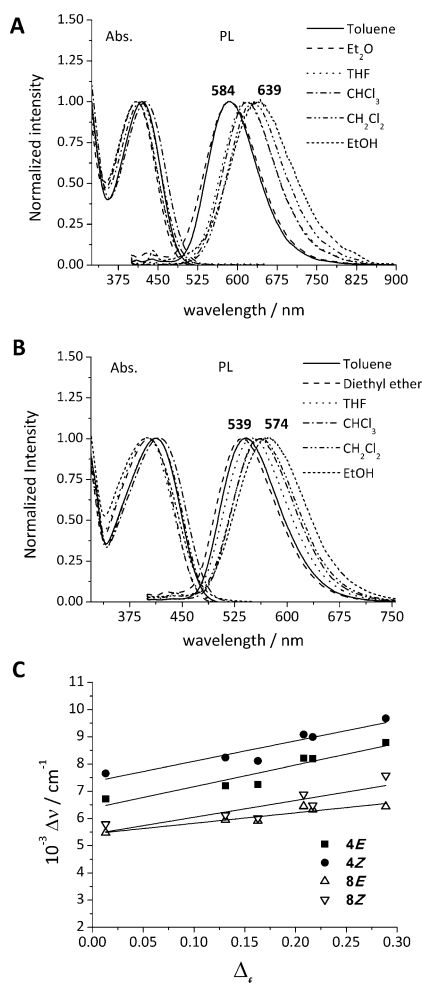


Figure 4. Absorption and fluorescence spectra (excited at 390 nm) for A) **4E** and B) **8Z** in different solvents. Interference spectra were removed for clarity. C) Lippert–Mataga plots for all dinitriles.

Supporting Information for **4Z** and **8E**. Although only small changes in the absorption spectra of the four dinitriles were observed, their emission spectra were significantly redshifted on increasing the solvent polarity from toluene to ethanol. The emission shift from 584 nm (toluene) to 639 nm (ethanol) for **4E**, for example, was enough to produce a visible color change in the solution from yellow to dark red (Figure S6 of the Supporting Information). However, **8E** and **8Z** showed an initial green fluorescence as a result of their blueshifted emission, and the visible color change was marginal compared to **4**. To quantify the solvatochromism of these compounds we used the Lippert–Mataga equation [Eq. (1)], which correlates the Stokes shift $\Delta\nu$ with the solvent polarity parameter Δf ^[15]

$$\Delta\nu = \nu_a - \nu_f = \frac{2\Delta f}{hca^3}(\mu_E - \mu_G)^2 + \text{constant} \quad (1)$$

where ν_a and ν_f are the absorption and fluorescence peak wavelengths, respectively, h is the Planck constant, c the speed of light, a the Onsager solvent cavity radius, and μ_E and μ_G are

the dipole moments in the excited and ground states, respectively. The calculation of the solvent polarity parameter is shown in Equation (S1) and all data are summarized in Table S1 (Supporting Information). The correlation plots between $\Delta\nu$ and Δf for the dinitriles (Figure 4C) show an ascendant linear tendency with increasing solvent polarity, that is, solvatochromicity. On linear fitting, large slopes were found for **4E** (7940) and **4Z** (7500), which represent stronger solvatochromism than for **8E** (3860), **8Z** (6180), and those reported for other donor–acceptor AIE-active chromophores.^[16] In addition, the larger Stokes shifts observed for **4** compared to **8** further push the emission towards the NIR region, and makes them more appropriate candidates for the design of NIR-emitting materials. The photophysical data of these dinitriles in solution showed that the control of the number of rotatable rings in these types of chromophore not only affects their AIE(E) output, but also can be used to fine-tune their emission profile and solvatochromic response.

Photophysical Properties in the Solid State

The AIEE behavior observed for the dinitriles in water/THF suggests that these compounds should also have strong fluorescence in the solid state. Indeed, the fluorescence spectra of dried powders of **4** and **8** showed a strong emission band in the 500–600 nm region, which is broader than in solution and extends further into the NIR region (Figure S7 of the Supporting Information). Their emission maxima and fluorescence quantum yields are summarized in Table 1.

Table 1. Emission wavelength maxima λ_{em} and absolute fluorescence quantum yields Φ_f of fluorophore samples with different morphologies.^[a]

| Compd. | As-obtained powder | | Pressed powder | | Fumed powder ^[b] | | Film ^[c] | | Aggregate ^[d] | |
|-----------|---------------------|--------------|---------------------|--------------|-----------------------------|--------------|---------------------|--------------|--------------------------|--------------|
| | λ_{em} [nm] | Φ_f [%] | λ_{em} [nm] | Φ_f [%] | λ_{em} [nm] | Φ_f [%] | λ_{em} [nm] | Φ_f [%] | λ_{em} [nm] | Φ_f [%] |
| 4E | 549 | 52.2 | 579 | 45.4 | 549 | 43.2 | 601 | 50.9 | 590 | 41.8 |
| 4Z | 587 | 47.9 | 599 | 43.7 | 579 | 55.5 | 613 | 44.7 | 637 | 33.7 |
| 8E | 576 | 52.3 | 580 | 59.9 | 560 | 57.9 | 569 | 28.9 | 564 | 26.9 |
| 8Z | 591 | 25.1 | 591 | 24.8 | 558 | 45.5 | 585 | 22.8 | 572 | 16.8 |

[a] Excitation at 390 nm. [b] Fumed with CHCl₃ for 3 min. [c] Prepared by dropping a concentrated solution of the dinitrile in CHCl₃ onto the substrate. [d] At a water fraction of 99%.

Photofunctional materials that respond to thermal, optical, and mechanical stimuli are promising for various applications.^[17] As shown in Figure 5 and Figure S8 of the Supporting Information, the emission band of **4E** powder underwent a 30 nm redshift from 549 to 579 nm on mechanical stimulus (grinding or manually pressing), which was enough to produce a visible color change in the powder from yellow to orange. When the pressed powder was exposed to CHCl₃ vapor for 3 min, the emission band blueshifted back to 549 nm, and the original yellow color was regenerated. Indeed, the color change was visible even during the first 10 s of exposure to

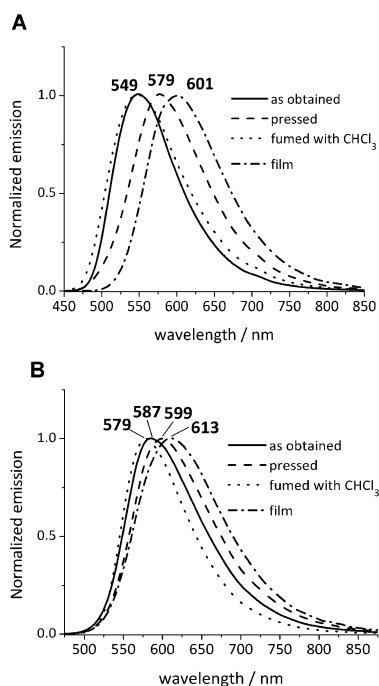


Figure 5. Changes in the fluorescence spectra of A) **4E** and B) **4Z** on external stimuli. Excitation at 365 nm.

CHCl_3 , and thus represents a rapid vapochromic response. Compound **4Z** showed a similar response, but the shift of the emission band on pressing/fuming was smaller (20 nm), and the color change was also less noticeable, mainly due to its longer emission wavelength compared to **4E**.

Exposure of the pressed powder to CHCl_3 , THF, and CH_2Cl_2 resulted in similar responses, whereas hexane and ethanol induced a weaker emission response (data not shown). Since the solubility of the dinitrile is much higher in the first three solvents than the last two, the fluorescence change may involve an interaction between **4E** and solvent molecules, rather than a response to solvent polarity.

We further investigated the fluorescence response of these luminophores on thermal treatment of their powders. As shown in Figure 6, heating pressed powders of **4E** and **4Z** at 140°C was also efficient for promoting reorganization of the molecular packing and consequently blueshifted their emission by 20–30 nm. For both pressurization/fuming and pressurization/heating cycles, the samples showed good reversibility and stability. The DPP-substituted dinitriles **8E** and **8Z** showed piezo- and vapochromic behavior as well, with a color change from orange (pressed powder) to yellow (fumed powder) under the same experimental conditions (Supporting Information, Figure S9). On the other hand, their emission response to thermal treatment was much poorer than those of **4E** and **4Z**. For **8E**, no changes were observed in the fluorescence band at 140°C , even after several minutes of heating, and at 210°C the emission maxima was shifted by only 12 nm. Compound **8Z** showed no thermal response, even on heating the sample near its melting point (190°C) for several minutes. The pressurization/fuming (**8E** and **8Z**) and pressurization/heating (**8E**) cycles were reversible, and no decomposition of the samples

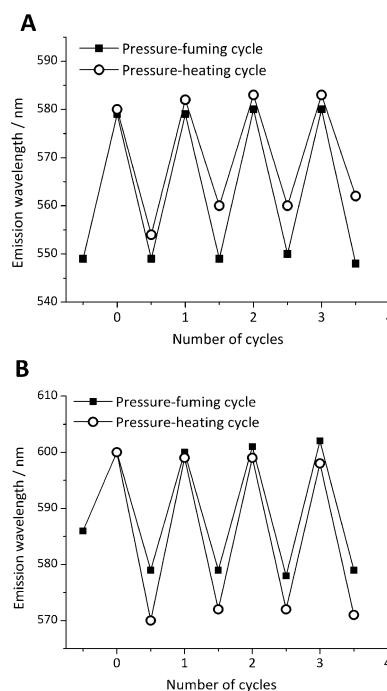


Figure 6. Reversibility of the fluorescence emission wavelength of A) **4E** and B) **4Z** on manual pressurization and fuming with CHCl_3 or heating at 140°C for 3 min.

was observed (Supporting Information, Figure S10). Interestingly, whereas the Φ_F values for the *E* isomers of **4** and **8** showed no significant change during the pressurization/fuming or pressurization/heating cycles, the values for the *Z* isomers were dependent on the crystallinity of the sample. As shown in Table 1 and Figure S10B (Supporting Information), **8Z** in particular showed a remarkable decrease in fluorescence from the fumed powder (45.5%) to the pressed powder (24.8%), which was also reversible on cycling. This is an example of crystallization-induced emission enhancement (CIEE), which has been observed for only a very limited number of compounds to date.^[18] Similarly to the pressed powders, thin films of the dinitriles (Figure 5 and Figure S8 in the Supporting Information) showed redshifted emission bands owing to their amorphous structure. A closer look at their fluorescence quantum yields (Table 1) reveals that the values decrease from **4E** to **8Z** with a similar trend to that observed for the aggregates in the water/THF mixtures, while the Φ_F values of the samples with the best crystallinity (fumed powders) are high for all fluorophores (43–58%). This indicates that the sample morphology, and thus the molecular packing, has a strict relationship with the position of the emission maxima and the fluorescence efficiency.

X-ray Crystal Structures

To gain further insight into the organization of the molecules in the solid state, single crystals of all the dinitriles were obtained for X-ray diffraction analysis. The X-ray structures of the dinitriles are shown in Figure 7. The phenyl rings in the TPE units of **4E** and **4Z** are oriented in a propeller-shaped manner,

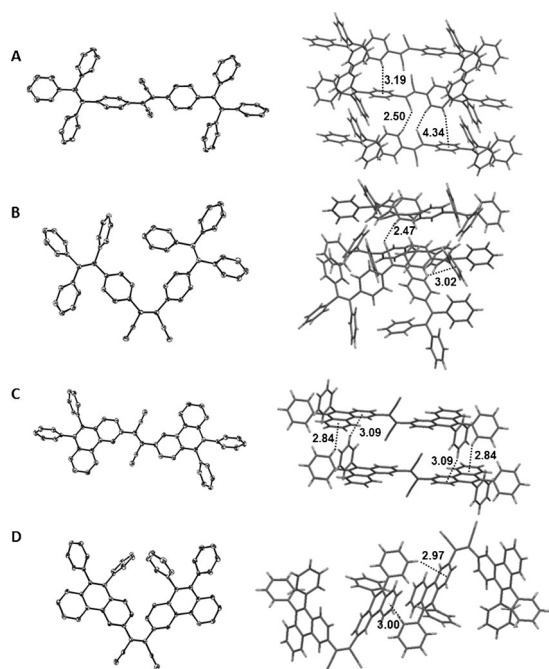


Figure 7. X-ray crystal structures (hydrogen atoms omitted) and packing diagrams of A) **4E**, B) **4Z**, C) **8E**, and D) **8Z**. The thermal ellipsoids are scaled to 50% probability. Solvent molecules are omitted for clarity.

with torsion angles varying between 41 and 63°. The phenyl rings connected to the central ethylene bridge are also twisted from its plane, by 28 and 34° for **4E** and **4Z**, respectively. This deviation from planarity leads to poorer overall conjugation in the molecule and explains why the crystalline samples show blueshifted emission compared to the amorphous state, in which the phenyl moieties are more free to rotate. The larger separation between the bulky TPE units in **4E** compared to **4Z** supports the premise that **4E** is more stable in solution. Compounds **8E** and **8Z** showed more pronounced distortions, with phenyl–phenanthrene torsion angles of 69–80° and phenanthrene–ethylene angles of 35 and 40°, respectively.

A closer look at the molecular structure of **8Z** also suggests the presence of intramolecular parallel-displaced π – π stacking^[19] between the phenanthrene units, with a centroid–centroid separation R_{cen} of 4.46 Å and parallel-displacement angle θ of 30° (Supporting Information, Scheme S2). This distance is even shorter than those found for anthracene-based aromatic compounds that show strong π – π interaction^[20] and results in an effective energetic contribution for this stereoisomer. Such interaction may account for the higher thermodynamic stability of **8Z** over **8E** in solution. No intermolecular π – π stacking was found in the packing structure of the dinitriles, owing to their twisted nature. However, intermolecular C–H... π and C–N...H interactions with distances of about 3.0 and 2.4 Å were observed, leading to locking of the phenyl rotors in the crystal. The absence of π – π stacking and blocking of the rotation of the phenyl rings are responsible for the strong fluorescence of these compounds in the crystalline state.

To further interpret the mechanochromic behavior, we conducted powder XRD measurements on **4E** (Supporting Infor-

mation, Figure S11). The as-obtained powder showed sharp reflection peaks due to its microcrystalline structure. On pressurization, the peaks became weaker and broader, and thus indicated a more amorphous character of the powder due to partial disruption of the molecular packing. After fuming with CHCl_3 for 3 min, the intensity and sharpness of the reflection peaks were regenerated, and this suggests that CHCl_3 molecules are effective in reordering the microcrystalline structure.

Finally, the mechanochromic applicability was demonstrated. The powder of **4E** was dispersed on filter paper, and the Chinese characters for “Tohoku University” were written by scratching the paper with a spatula (Supporting Information, Figure S12). Under UV irradiation, the yellow background fluorescence and the orange emission from the characters produced strong contrast for a clear image of the written content. On fuming the paper with CHCl_3 or CH_2Cl_2 , or heating it at 140 °C for 5 min, the crystallinity of the scratched powder was regenerated and the letters became invisible under UV light. This writing/erasing process could be repeated reversibly without decomposition of the chromophore, and thus the dinitriles have potential applications for rewritable data storage, sensing, and security printing.^[21]

Conclusion

Modification of the blue-emitting TPE and DPP moieties with electron-withdrawing cyano groups and vinylene linkages yielded dinitriles **4** and **8** as pure *E/Z* isomers, which exhibited redshifted absorption and emission bands as well as large Stokes shifts. The *E/Z* isomerization experiments in solution showed that the number of rotatable phenyl groups in the dinitriles determines the *E/Z* interconversion kinetics and thermodynamic stability of the stereoisomers due to the difference in the bulkiness of the groups and the presence or absence of intramolecular interactions. TPE-substituted dinitrile **4** showed more pronounced fluorescence enhancement on aggregation (12-fold increase) as well as larger Stokes shifts and solvatochromism compared to **8**. On grinding or pressurization of the powder samples of **4** and **8**, their emission bands were redshifted by about 20–30 nm, which was enough to produce a visible color change from yellow to orange (mechano/piezochromism). Fuming the powders for several seconds was enough to regenerate their original yellow color (vapochromism). Moreover, heating the samples for several minutes also blueshifted their fluorescence emission (thermochromism). This shows that the molecular organization in the packing structure has a critical influence on the fluorescence response. Interestingly, **8Z** is a rare example of CIEE, which demonstrates that completely different properties may arise from stereoisomers of a single AIE-active fluorophore. The AIEE behavior and the various chromic responses observed for **4** and **8** make them potential candidates for the design of smart materials for various purposes.

Experimental Section

Instrumentation

^1H NMR and ^{13}C NMR spectra were obtained on a Bruker AVANCE III 500 spectrometer. The spectra were referenced to the residual solvent proton peaks as internal standard. MALDI-TOF mass spectra were obtained on an AB Sciex 4800Plus TOF/TOF Analyzer. Electronic absorption spectra and fluorescence spectra were recorded on JASCO V-570 and HITACHI F-4500 spectrophotometers, respectively. Absolute fluorescence quantum yields were measured by using a Hamamatsu C9920-03G calibrated integrating-sphere system.

Materials and Methods

All solvents and reagents were used without purification unless otherwise specified. Dehydrated DMSO was purchased from Wako Pure Chemicals Industries Ltd., and CH_2Cl_2 and CCl_4 were distilled from CaH_2 and stored over molecular sieves prior to use. *N*-Bromosuccinimide (NBS) was recrystallized by slow cooling of a saturated solution in boiling water. Compounds **1**, **2**, and **5** were synthesized according to previous literature.^[13,22] The isomerization experiments were conducted by using NMR tubes containing 4.5 mm solutions of pure **4E/4Z** or **8E/8Z** in CDCl_3 . The tubes were placed 5 cm from a UV lamp (365 nm, 9.0 W) and were irradiated for 4 h, during which the ^1H NMR spectra were recorded at defined intervals. The THF/water experiments were performed by preparing a 1.0 mM stock solution of samples in THF and adding 20 μL of this solution to each THF/water mixture with a final volume of 3 mL. After homogenizing the solution, the fluorescence quantum yields were measured immediately.

Synthesis

2-[4-(1,2,2-Triphenylvinyl)phenyl]acetonitrile (3): In a round-bottom flask, potassium cyanide (247 mg, 3.8 mmol) was dissolved in dehydrated DMSO (20 mL) at 90 °C. Compound **2** (1.5 g, 3.5 mmol) was then added to the mixture, which was stirred at the same temperature for 2 h. After cooling the flask to room temperature, the reaction mixture was poured into water (100 mL) and extracted with ethyl acetate. The organic layers were collected, dried over MgSO_4 , and the solvent removed. Purification by silica-gel column chromatography with CHCl_3 /hexane (9/1 v/v) as eluent yielded the pure compound as a yellow powder. Yield: 814 mg, 63%. ^1H NMR in CDCl_3 : δ = 7.09–6.98 (m, 19H), 3.64 ppm (s, 2H).

2,3-Bis[4-(1,2,2-triphenylvinyl)phenyl]but-2-ene dinitrile (4): Sodium methoxide (Na, 62 mg, 2.68 mmol) in methanol (3 mL) solution was added dropwise to a mixture of **3** (500 mg, 1.34 mmol), I_2 (339 mg, 1.34 mmol), and diethyl ether (8 mL) over 20 min with stirring at 0 °C. The mixture was allowed to react for 30 min, filtered, and washed with cold methanol to remove any excess of iodine. The title compound was obtained as a mixture of regioisomers (**4E** and **4Z**, 240 mg, 49%). Finally, **4E** and **4Z** were separated by silica-gel column chromatography with CHCl_3 as eluent. To avoid isomerization, solutions of pure isomers were protected from light exposure during all procedures. **4Z**: m.p. 210–215 °C; MALDI-TOF-MS: m/z calcd for $[\text{M}]^+$: 738.31; found: 738.39; ^1H NMR in CDCl_3 : δ = 7.13–6.94 ppm (m, 38H). **4E**: m.p. 257 °C; MALDI-TOF-MS: m/z found: 738.40. ^1H NMR in CDCl_3 : δ = 7.53 (d, 4H), 7.14–7.08 (m, 22H), 7.03–7.00 ppm (m, 12H).

3-(Bromomethyl)-9,10-diphenylphenanthrene (6): Compound **5** (1.0 g, 3.0 mmol), NBS (622 mg, 3.5 mmol), and benzoyl peroxide (7 mg, 0.03 mmol) were heated to reflux in CCl_4 (60 mL) for 12 h,

and then the reaction mixture was quenched with saturated aqueous $\text{Na}_2\text{S}_2\text{O}_3$. The organic layer was washed with water, dried over MgSO_4 , filtered, and concentrated. The crude product was purified by silica-gel column chromatography with CHCl_3 /hexane (1/2 v/v) as eluent. Yield: 900 mg, 71%. MALDI-TOF-MS: m/z calcd for $[\text{M}]^+$: 422.1; found: 422.9; ^1H NMR in CDCl_3 : δ = 8.80 (s, 1H), 8.79 (d, J = 5.5 Hz, 1H), 7.69 (m, 2H), 7.53 (m, 4H), 7.25–7.12 (m, 9H), 4.78 ppm (s, 2H); ^{13}C NMR in CDCl_3 : δ = 139.36, 137.96, 136.96, 135.69, 132.14, 131.77, 131.01, 130.08, 129.73, 128.66, 127.99, 127.67, 127.38, 126.96, 126.63, 123.03, 122.51, 34.19 ppm.

2-(9,10-Diphenylphenanthren-3-yl)acetonitrile (7): In a round-bottom flask, KCN (182 mg, 2.8 mmol) was dissolved in DMSO (10 mL) at 90 °C. Compound **6** (600 mg, 1.4 mmol) and NaI (104.9 mg, 0.71 mmol) were then added to the flask and the mixture allowed to react for 3 h. After cooling to room temperature, the mixture was poured into 100 mL of saturated aqueous NaHCO_3 and extracted with CHCl_3 . The organic layer was concentrated and the crude product purified by silica-gel column chromatography with CH_2Cl_2 /hexane as eluent. Yield: 326 mg, 63%. MALDI-TOF-MS: m/z calcd for $[\text{M}]^+$: 369.1; found: 369.0. ^1H NMR in CDCl_3 : δ = 8.80 (d, J = 8.5 Hz, 1H), 8.76 (s, 1H), 7.70 (td, 1H), 7.57 (d, J = 8.0 Hz, 1H), 7.52 (d, J = 7.0 Hz, 1H), 7.48 (d, J = 7.0 Hz, 1H), 7.39 (dd, 1H), 7.24–7.12 (m, 10H), 4.03 ppm (s, 2H); ^{13}C NMR in CDCl_3 : δ = 139.26, 137.88, 136.82, 132.22, 131.82, 131.47, 130.98, 130.35, 129.48, 128.93, 128.01, 127.71, 127.17, 126.72, 126.12, 122.51, 121.86, 117.95, 24.10 ppm.

2,3-Bis(9,10-diphenylphenanthren-3-yl)but-2-enedinitrile (8): Compound **7** (100 mg, 0.27 mmol), I_2 (68.7 mg, 0.27 mmol), and THF (5 mL) were placed in a round-bottom flask and cooled to –35 °C. Sodium methoxide (Na 14 mg, 0.6 mmol) in methanol solution (1 mL) was then added dropwise to the stirred mixture, which was left to react for further 10 min. The mixture was diluted with CHCl_3 , washed with saturated aqueous $\text{Na}_2\text{S}_2\text{O}_3$, and the organic layer collected and dried over MgSO_4 . The *E* and *Z* isomers were isolated by silica-gel chromatography with CHCl_3 /hexane (9/1) as eluent. Yield: 14 mg of **8E** (14%) and 10 mg of **8Z** (10%). **8E**: m.p. > 300 °C; MALDI-TOF-MS: m/z calcd for $[\text{M}]^+$: 734.27; found: 734.13; ^1H NMR in CDCl_3 : δ = 9.42 (s, 2H), 8.90 (d, J = 8.4 Hz, 2H), 8.00 (d, J = 8.6 Hz, 2H), 7.74 (t, 4H), 7.61 (d, J = 7.5 Hz, 2H), 7.56 (t, 2H), 7.28–7.22 (m, 12H), 7.19–7.17 ppm (m, 8H). **8Z**: m.p. 190–195 °C. MALDI-TOF-MS: m/z found: 734.15; ^1H NMR in CDCl_3 : δ = 8.95 (s, 2H), 8.47 (d, J = 8.2 Hz, 2H), 7.60 (t, 2H), 7.56 (d, J = 6.9 Hz, 2H), 7.52 (d, J = 7.0 Hz, 2H), 7.40 (d, J = 8.7 Hz, 2H), 7.36 (d, 2H), 7.23–7.10 (m, 16H), 7.03 ppm (m, 4H).

Acknowledgements

This work was partly supported by a Grant-in-Aids for Scientific Research on Innovative Areas (25109502, "Stimuli-responsive Chemical Species"), Scientific Research (B) (No. 23350095), Challenging Exploratory Research (No. 25620019), and Young Scientist (B) (No. 24750031) from the Ministry of Education, Culture, Sports, Science, and Technology (MEXT). The authors thank Prof. Takeaki Iwamoto and Dr. Shintaro Ishida (Tohoku University) for the single-crystal X-ray measurements, and Dr. Eunsang Kwon (Tohoku University) for the powder X-ray measurements. Some of the calculations were performed by using supercomputing resources at the Cyberscience Center of Tohoku University.

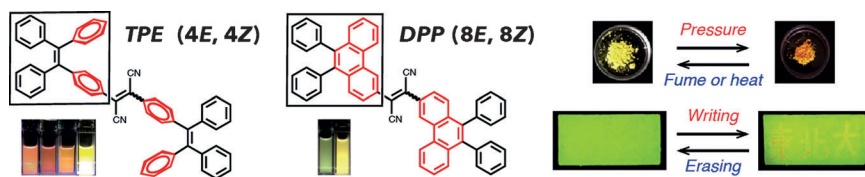
Keywords: aggregation · cyanides · dyes/pigments · fluorescence · solvatochromism

- [1] a) M.-E. Ragoussi, M. Ince, T. Torres, *Eur. J. Org. Chem.* **2013**, 6475–6489; b) C. Qin, W.-Y. Wong, L. Han, *Chem. Asian J.* **2013**, 8, 1706–1719; c) S. Mori, M. Nagata, Y. Nakahata, K. Yasuta, R. Goto, M. Kimura, M. Taya, *J. Am. Chem. Soc.* **2010**, 132, 4054–4055; d) G. de La Torre, C. G. Claessens, T. Torres, *Chem. Commun.* **2007**, 2000–2015.
- [2] a) S. K. Yen, D. Jańczewski, J. Lakshmi, S. Dolmanan, S. Tripathy, V. Ho, V. Vijayaragavan, A. Hariharan, P. Padmanabhan, K. Bhakoo, T. Sudhaharan, S. Ahmed, Y. Zhang, S. T. Selvan, *ACS Nano* **2013**, 7, 6796–6805; b) J. O. Escobedo, O. Rusin, S. Lim, R. M. Strongin, *Curr. Opin. Chem. Biol.* **2010**, 14, 64–70.
- [3] a) J. F. Lovell, T. W. B. Liu, J. Chen, G. Zheng, *Chem. Rev.* **2010**, 110, 2839–2857; b) S. Atilgan, Z. Ekmekci, A. L. Dogan, D. Guc, E. U. Akkaya, *Chem. Commun.* **2006**, 4398–4400.
- [4] a) J. E. Anthony, *Angew. Chem. Int. Ed.* **2008**, 47, 452–483; *Angew. Chem.* **2008**, 120, 460–492; b) G. E. Rudebusch, A. G. Fix, H. A. Henthorn, C. L. Vonnegut, L. N. Zakharov, M. M. Haley, *Chem. Sci.* **2014**, 5, 3627–3633; c) T. Furuyama, Y. Ogura, K. Yoza, N. Kobayashi, *Angew. Chem. Int. Ed.* **2012**, 51, 11110–11114; *Angew. Chem.* **2012**, 124, 11272–11276.
- [5] a) K. Kurotobi, Y. Toude, K. Kawamoto, Y. Fujimori, S. Ito, P. Chabera, V. Sundström, H. Imahori, *Chem. Eur. J.* **2013**, 19, 17075–17081; b) A. Yella, H.-W. Lee, H. N. Tsao, C. Yi, A. K. Chandiran, M. Nazeeruddin, E. W.-G. Diau, C.-Y. Yeh, S. M. Zakeeruddin, M. Grätzel, *Science* **2011**, 334, 629–634.
- [6] a) Y. Hong, J. W. Y. Lam, B. Z. Tang, *Chem. Soc. Rev.* **2011**, 40, 5361–5388; b) T. T. Tasso, Y. Yamasaki, T. Furuyama, N. Kobayashi, *Dalton Trans.* **2014**, 43, 5886–5892.
- [7] J. Luo, Z. Xie, J. W. Y. Lam, L. Cheng, H. Chen, C. Qiu, H. S. Kwok, X. Zhan, Y. Liu, D. Zhu, B. Z. Tang, *Chem. Commun.* **2001**, 1740–1741.
- [8] J. Mei, Y. Hong, J. W. Y. Lam, A. Qin, Y. Tang, B. Z. Tang, *Adv. Mater.* **2014**, 1–51.
- [9] a) G. Mu, W. Zhang, P. Xu, H. Wang, Y. Wang, L. Wang, S. Zhuang, X. Zhu, *J. Phys. Chem. C* **2014**, 118, 8610–8616; b) R. Hu, J. W. Y. Lam, Y. Liu, X. Zhang, B. Z. Tang, *Chem. Eur. J.* **2013**, 19, 5617–5624; c) Y. Liu, Y. Lv, H. Xi, X. Zhang, S. Chen, J. W. Y. Lam, R. T. K. Kwok, F. Mahtab, H. S. Kwok, X. Tao, B. Z. Tang, *Chem. Commun.* **2013**, 49, 7216–7218.
- [10] a) J. Shi, N. Chang, C. Li, J. Mei, C. Deng, X. Luo, Z. Liu, Z. Bo, Y. Q. Dong, B. Z. Tang, *Chem. Commun.* **2012**, 48, 10675–10677; b) X. Gao, Q. Peng, Y. Niu, D. Wang, Z. Shuai, *Phys. Chem. Chem. Phys.* **2012**, 14, 14207–14216.
- [11] a) J. Wang, J. Mei, R. Hu, J. Z. Sun, A. Qin, B. Z. Tang, *J. Am. Chem. Soc.* **2012**, 134, 9956–9966; b) X. Y. Shen, Y. J. Wang, E. Zhao, W. Z. Yuan, Y. Liu, P. Lu, A. Qin, Y. Ma, J. Z. Sun, B. Z. Tang, *J. Phys. Chem. C* **2013**, 117, 7334–7347.
- [12] H.-C. Yeh, W.-C. Wu, Y.-S. Wen, D.-C. Dai, J.-K. Wang, C.-T. Chen, *J. Org. Chem.* **2004**, 69, 6455–6462.
- [13] T. S. Navale, K. Thakur, R. Rathore, *Org. Lett.* **2011**, 13, 1634–1637.
- [14] a) C. Baik, Z. M. Hudson, H. Amarné, S. Wang, *J. Am. Chem. Soc.* **2009**, 131, 14549–14559; b) T. Arai, T. Karatsu, H. Sakuragi, K. Tokumaru, *Tetrahedron Lett.* **1983**, 24, 2873–2876.
- [15] J. R. Lakowicz, *Principles of Fluorescence Spectroscopy*, Springer, Baltimore, **2006**.
- [16] a) Y. Zhang, T. Han, S. Gu, T. Zhou, C. Zhao, Y. Guo, X. Feng, B. Tong, J. Bing, J. Shi, J. Zhi, Y. Dong, *Chem. Eur. J.* **2014**, 20, 8856–8861; b) J. Mei, J. Wang, J. Z. Sun, H. Zhao, W. Yuan, C. Deng, S. Chen, H. H. Y. Sung, P. Lu, A. Qin, H. S. Kwok, Y. Ma, I. D. Williams, B. Z. Tang, *Chem. Sci.* **2012**, 3, 549–558; c) J. Tong, Y. Wang, J. Mei, J. Wang, A. Qin, J. Z. Sun, B. Z. Tang, *Chem. Eur. J.* **2014**, 20, 4661–4670.
- [17] Y. Sagara, T. Kato, *Nat. Chem.* **2009**, 1, 605–610.
- [18] a) R. Yoshii, A. Hirose, K. Tanaka, Y. Chujo, *J. Am. Chem. Soc.* **2014**, 136, 18131–18139; b) R. Yoshii, A. Hirose, K. Tanaka, Y. Chujo, *Chem. Eur. J.* **2014**, 20, 8320–8324.
- [19] a) G. B. McGaughey, M. Gagné, A. K. Rappé, *J. Biol. Chem.* **1998**, 273, 15458–15463; b) R.-F. Dou, X.-C. Ma, L. Xi, H. L. Yip, K. Y. Wong, W. M. Lau, J.-F. Jia, Q.-K. Xue, W.-S. Yang, H. Ma, A. K. Y. Jen, *Langmuir* **2006**, 22, 3049–3056.
- [20] F. Li, N. Gao, H. Xu, W. Liu, H. Shang, W. Yang, M. Zhang, *Chem. Eur. J.* **2014**, 20, 9991–9997.
- [21] a) H. Moustroph, M. Stollenwerk, V. Bressau, *Angew. Chem. Int. Ed.* **2006**, 45, 2016–2035; *Angew. Chem.* **2006**, 118, 2068–2087; b) J. Wu, W. Liu, J. Ge, H. Zhang, P. Wang, *Chem. Soc. Rev.* **2011**, 40, 3483–3495; c) A. Kishimura, T. Yamashita, K. Yamaguchi, T. Aida, *Nat. Mater.* **2005**, 4, 546–549.
- [22] H. Shi, R. T. K. Kwok, J. Liu, B. Xing, B. Z. Tang, B. Liu, *J. Am. Chem. Soc.* **2012**, 134, 17972–17981.

Received: November 18, 2014

Published online on ■■■■■, 0000

FULL PAPER



What it takes to shine: Dinitriles bearing tetraphenylethylene (TPE) or diphenylphenanthrene (DPP) units showed distinct aggregation-induced emission (AIE) and various reversible chromic re-

sponses to external stimuli (solvato-, piezo-, vapo-, and thermochromism), depending on the isomer conformation and number of rotatable phenyl rings in the molecule.

Aggregation-Induced Emission

T. T. Tasso, T. Furuyama, N. Kobayashi*



Dinitriles Bearing AIE-Active Moieties: 
Synthesis, *E/Z* Isomerization, and
Fluorescence Properties